Electronic Supplementary Material (ESI) for Dalton Transactions.

I. Crystal structure description

Table S1. Selected bond lengths, the shortest interatomic distances *d* (Å) and angles *ω* (°) for $\mathbf{1_{Gd}}$.

Bond/Distance	*d*	Bond/Distance	*d*
Gd1–O8^i	2.347(3)	Gd1–O4	2.510(3)
Gd1–O5	2.368(3)	Gd1–O1	2.575(3)
Gd1–O1W	2.404(3)	Cu1–O7	1.919(3)
Gd1–O9^i	2.417(3)	Cu1–O6	1.926(3)
Gd1–O3	2.444(3)	Cu1–O9	1.962(3)
Gd1–O2W	2.468(3)	Cu1–O9^i	1.974(3)
Gd1–O2	2.479(3)	Cu1···Cu1^i	3.0449(12)
Angle	*ω*	Angle	*ω*
O8^i–Gd1–O5	144.48(11)	O8^i–Gd1–O4	74.24(12)
O8^i–Gd1–O1W	142.08(12)	O5–Gd1–O4	73.30(12)
O5–Gd1–O1W	71.49(12)	O1W–Gd1–O4	126.89(13)
O8^i–Gd1–O9^i	77.54(10)	O9^i–Gd1–O4	67.99(9)
O5–Gd1–O9^i	77.26(10)	O3–Gd1–O4	52.50(10)
O1W–Gd1–O9^i	136.89(10)	O2W–Gd1–O4	115.88(12)
O8^i–Gd1–O3	92.07(12)	O2–Gd1–O4	139.29(12)
O5–Gd1–O3	79.42(11)	O8^i–Gd1–O1	119.48(11)
O1W–Gd1–O3	82.71(12)	O5–Gd1–O1	73.91(10)
O9^i–Gd1–O3	120.02(10)	O1W–Gd1–O1	73.09(11)
O8^i–Gd1–O2W	71.99(12)	O9^i–Gd1–O1	70.18(9)
O5–Gd1–O2W	136.61(11)	O3–Gd1–O1	148.42(10)
O1W–Gd1–O2W	70.29(12)	O2W–Gd1–O1	112.87(12)
O9^i–Gd1–O2W	146.13(11)	O2–Gd1–O1	50.97(10)
O3–Gd1–O2W	76.12(11)	O4–Gd1–O1	131.15(10)
O8^i–Gd1–O2	74.50(12)	O7–Cu1–O6	89.25(13)
O5–Gd1–O2	124.71(11)	O7–Cu1–O9	96.54(12)
O1W–Gd1–O2	93.68(13)	O6–Cu1–O9	167.27(13)
O9^i–Gd1–O2	80.31(11)	O7–Cu1–O9^i	172.51(13)
O3–Gd1–O2	153.18(11)	O6–Cu1–O9^i	96.63(12)
O2W–Gd1–O2	77.65(12)	O9–Cu1–O9^i	78.64(12)

Symmetry code: (i) -*x*+1, -*y*+1, -*z*+1.

Table S2. Hydrogen bonding parameters of structure $\mathbf{1_{Gd}}$.

Fragment D–H···A	Distance/ Å			D–H···A /°
	D–H	H···A	D···A	
O1–H1WB···O1S	0.88	1.85	2.698(6)	159.3
O1W–H1WA···O3^i	0.86	1.82	2.635(4)	157.3
O2W–H2WB···O1W^i	0.81	2.37	3.140(5)	159.4
O2W–H2WA···O2S	0.76	2.08	2.721(7)	142.3
O1S–H1SO···O1	0.99	1.73	2.712(5)	177.8
O2S–H2SO···O2	0.95	1.90	2.766(7)	150.0

Symmetry code: (i) -*x*, -*y*+1, -*z*+1.

Table S3. Selected bond lengths, the shortest interatomic distances *d* (Å) and angles *ω* (°) for **2**$_{\mathbf{Dy}}$.

Bond/Distance	*d*	Bond/Distance	*d*
Dy1–O10^{i}	2.337(2)	Cu1–O9	1.942(2)
Dy1–O7	2.441(2)	Na1–O5^{ii}	2.652(3)
Dy1–O1^{ii}	2.442(2)	Na1–O2	2.254(3)
Dy1–O5	2.254(2)	Na1–O4^{ii}	2.370(3)
Dy1–O8	2.310(2)	Na1–O4	2.238(3)
Dy1–O12^{i}	2.327(2)	Na1–O3	2.277(5)
Dy1–O6	2.436(3)	Dy1···Cu1	3.5090(5)
Dy1–O2^{ii}	2.452(2)	Dy1···Cu1^{i}	3.5104(6)
Cu1–O10	1.966(2)	Dy1···Na1^{ii}	3.7301(14)
Cu1–O10^{i}	1.969(2)	Cu1···Cu1^{i}	3.0371(8)
Cu1–O11	1.947(2)	Na1···Na1^{ii}	3.366(3)
Angle	*ω*	Angle	*ω*
O10^{i}–Dy1–O7	76.69(8)	O8–Dy1–O1^{ii}	143.31(8)
O10^{i}–Dy1–O1^{ii}	77.11(8)	O8–Dy1–O12^{i}	114.16(9)
O10^{i}–Dy1–O6	128.04(8)	O8–Dy1–O6	82.33(10)
O10^{i}–Dy1–O2^{ii}	127.15(10)	O8–Dy1–O2^{ii}	157.68(9)
O7–Dy1–O2^{ii}	100.78(9)	O12^{i}–Dy1–O10^{i}	74.42(8)
O1^{ii}–Dy1–O7	73.33(8)	O12^{i}–Dy1–O7	143.83(8)
O1^{ii}–Dy1–O6	97.54(10)	O12^{i}–Dy1–O1^{ii}	79.35(9)
O1^{ii}–Dy1–O2^{ii}	52.85(8)	O12^{i}–Dy1–O6	156.43(9)
O5–Dy1–O10^{i}	140.73(9)	O12^{i}–Dy1–O2^{ii}	80.30(10)
O5–Dy1–O7	133.31(9)	O6–Dy1–O7	52.98(9)
O5–Dy1–O1^{ii}	129.60(8)	O6–Dy1–O2^{ii}	79.37(10)
O5–Dy1–O8	86.87(9)	O10–Cu1–O10^{i}	78.96(10)
O5–Dy1–O12^{i}	82.61(9)	O11–Cu1–O10	94.92(11)
O5–Dy1–O6	81.61(9)	O11–Cu1–O10^{i}	171.59(10)
O5–Dy1–O2^{ii}	77.95(9)	O9–Cu1–O10^{i}	95.05(9)
O8–Dy1–O10^{i}	74.55(8)	O9–Cu1–O10	171.47(11)
O8–Dy1–O7	77.82(9)	O9–Cu1–O11	91.55(10)

Symmetry codes: (i) -*x*+1, -*y*+1, -*z*; (ii) -*x*+1, -*y*+2, -*z*+1.

Table S4. Hydrogen bonding parameters of structure **2**$_{\mathbf{Dy}}$.

Fragment D–H···A	Distance/ Å			D–H···A /°
	D–H	H···A	D···A	
O3–H3···O6^{i}	0.82	1.94	2.727(5)	161
O10–H10···O13	0.72	2.04	2.701(9)	154
O10–H10···O13A	0.72	2.05	2.727(11)	158

Symmetry codes: (i) 1-x, 2-y, 1-z.

Table S5. Selected bond lengths, the shortest interatomic distances *d* (Å) and angles *ω* (°) for $\mathbf{2_{Gd}}$.

Bond/Distance	*d*	Bond/Distance	*d*
Gd1–O5	2.288(3)	Cu1–O9	1.947(3)
Gd1–O6	2.467(4)	Na1–O5^{i}	2.572(4)
Gd1–O10	2.364(3)	Na1–O4^{i}	2.385(4)
Gd1–O1^{i}	2.471(3)	Na1–O4	2.226(4)
Gd1–O8	2.348(3)	Na1–O2	2.238(4)
Gd1–O7	2.451(3)	Na1–O3	2.265(5)
Gd1–O12^{ii}	2.336(3)	Gd1···Cu1	3.501(3)
Gd1–O2^{i}	2.483(3)	Gd1···Cu1^{ii}	3.502(3)
Cu1–O10	1.965(3)	Gd1···Na1^{i}	3.704(3)
Cu1–O10^{ii}	1.978(3)	Cu1···Cu1^{ii}	3.061(3)
Cu1–O11	1.948(3)	Na1···Na1^{i}	3.352(3)
Angle	*ω*	Angle	*ω*
O5–Gd1–O6	81.35(12)	O8–Gd1–O7	143.21(11)
O5–Gd1–O10	141.84(10)	O8–Gd1–O2^{i}	79.26(13)
O5–Gd1–O1^{i}	129.06(11)	O7–Gd1–O6	52.99(11)
O5–Gd1–O8	83.54(12)	O7–Gd1–O1^{i}	73.40(11)
O5–Gd1–O7	132.96(11)	O7–Gd1–O2^{i}	101.88(13)
O5–Gd1–O12^{ii}	87.24(11)	O12^{ii}–Gd1–O6	82.37(12)
O5–Gd1–O2^{i}	77.25(11)	O12^{ii}–Gd1–O10	74.82(11)
O6–Gd1–O1^{i}	96.58(12)	O12^{ii}–Gd1–O1^{i}	143.31(9)
O6–Gd1–O2^{i}	79.66(12)	O12^{ii}–Gd1–O8	115.08(12)
O10–Gd1–O6	127.60(11)	O12^{ii}–Gd1–O7	77.12(12)
O10–Gd1–O1^{i}	77.23(11)	O12^{ii}–Gd1–O2^{i}	157.77(11)
O10–Gd1–O7	75.97(12)	O10–Cu1–O10^{ii}	78.16(13)
O10–Gd1–O2^{i}	126.90(10)	O11–Cu1–O10^{ii}	96.09(13)
O1^{i}–Gd1–O2^{i}	52.68(10)	O11–Cu1–O10	172.01(12)
O8–Gd1–O6	156.30(10)	O9–Cu1–O10^{ii}	171.34(11)
O8–Gd1–O10	74.54(11)	O9–Cu1–O10	95.25(13)
O8–Gd1–O1^{i}	79.01(11)	O9–Cu1–O11	90.99(13)

Symmetry codes: (i) -*x*+1, -*y*+1, -*z*+1; (ii) -*x*+1, -*y*+2, -*z*+2.

Table S6. Hydrogen bonding parameters of structure $\mathbf{2_{Gd}}$.

Fragment D–H···A	Distance/ Å			D–H···A /°
	D–H	H···A	D···A	
O3–H3···O6^{i}	0.98	1.85	2.725(6)	148
O10–H10···O13A	0.76	1.99	2.719(10)	161
O10–H10···O13B	0.76	1.92	2.670(15)	165

Symmetry codes: (i) 1-x, 1-y, 1-z.

Table S7. Selected bond lengths, the shortest interatomic distances *d* (Å) and angles *ω* (°) for $\mathbf{2_{Tb}}$.

Bond/Distance	*d*	Bond/Distance	*d*
Tb1–O1^{i}	2.465(3)	Cu1–O10^{ii}	1.982(2)
Tb1–O10	2.342(3)	Cu1–O7^{ii}	2.432(4)
Tb1–O5	2.265(3)	Na1–O5^{i}	2.576(4)
Tb1–O7	2.426(3)	Na1–O2	2.240(4)
Tb1–O8	2.335(3)	Na1–O3	2.280(4)
Tb1–O12^{ii}	2.317(3)	Na1–O4^{i}	2.381(3)
Tb1–O2^{i}	2.457(3)	Tb1···Cu1	3.4931(8)
Tb1–O6	2.455(3)	Tb1···Cu1^{ii}	3.4844(7)
Cu1–O9	1.948(3)	Tb1···Na1^{i}	3.699(2)
Cu1–O11	1.948(3)	Cu1···Cu1^{ii}	3.0550(9)
Cu1–O10	1.970(3)	Na1···Na1^{i}	3.344(2)
Angle	*ω*	Angle	*ω*
O10–Tb1–O1^{i}	77.32(10)	O12^{ii}–Tb1–O1^{i}	143.05(9)
O10–Tb1–O7	75.58(10)	O12^{ii}–Tb1–O10	75.02(10)
O10–Tb1–O2^{i}	126.78(10)	O12^{ii}–Tb1–O7	76.71(10)
O10–Tb1–O6	127.52(10)	O12^{ii}–Tb1–O8	115.63(11)
O5–Tb1–O1^{i}	129.39(10)	O12^{ii}–Tb1–O2^{i}	157.74(11)
O5–Tb1–O10	141.82(11)	O12^{ii}–Tb1–O6	82.47(11)
O5–Tb1–O7	133.10(11)	O2^{i}–Tb1–O1^{i}	52.83(10)
O5–Tb1–O8	83.53(10)	O6–Tb1–O1^{i}	95.63(11)
O5–Tb1–O12^{ii}	87.03(10)	O6–Tb1–O2^{i}	79.75(11)
O5–Tb1–O2^{i}	77.23(10)	O9–Cu1–O10^{ii}	171.80(12)
O5–Tb1–O6	81.55(11)	O9–Cu1–O10	94.95(11)
O7–Tb1–O1^{i}	73.02(9)	O9–Cu1–O7^{ii}	93.32(12)
O7–Tb1–O2^{i}	102.65(10)	O11–Cu1–O9	91.20(11)
O7–Tb1–O6	53.13(11)	O11–Cu1–O10	171.83(13)
O8–Tb1–O1^{i}	79.42(9)	O11–Cu1–O10^{ii}	95.59(11)
O8–Tb1–O10	74.82(10)	O11–Cu1–O7^{ii}	88.98(12)
O8–Tb1–O7	143.12(10)	O10–Cu1–O10^{ii}	78.75(11)

Symmetry codes: (i) -*x*+1, -*y*+1, -*z*+1; (ii) -*x*+1, -*y*, -*z*.

Table S8. Hydrogen bonding parameters of structure $\mathbf{2_{Tb}}$.

Fragment D–H···A	Distance/ Å			D–H···A /°
	D–H	H···A	D···A	
O3–H3···O6^{i}	0.84	1.94	2.728(6)	156
O10–H10···O13A	0.87	1.86	2.706(7)	165
O10–H10···O13B	0.87	1.83	2.67(2)	162

Symmetry codes: (i) 1-x, 1-y, 1-z.

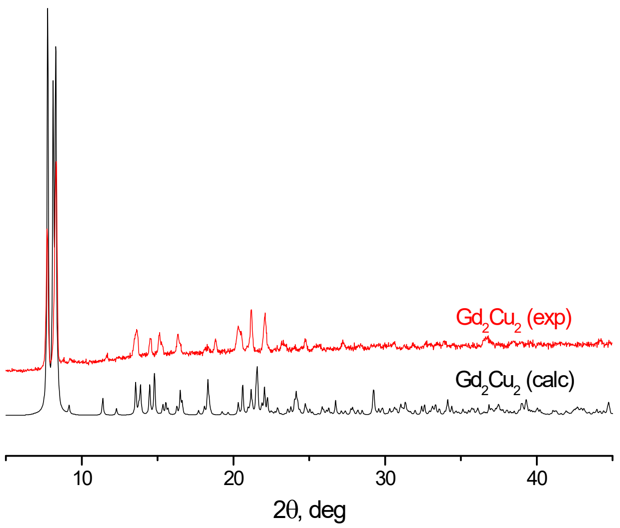
Gd$_2$Cu$_2$ (exp)
Gd$_2$Cu$_2$ (calc)
10
20
30
40
2θ, deg

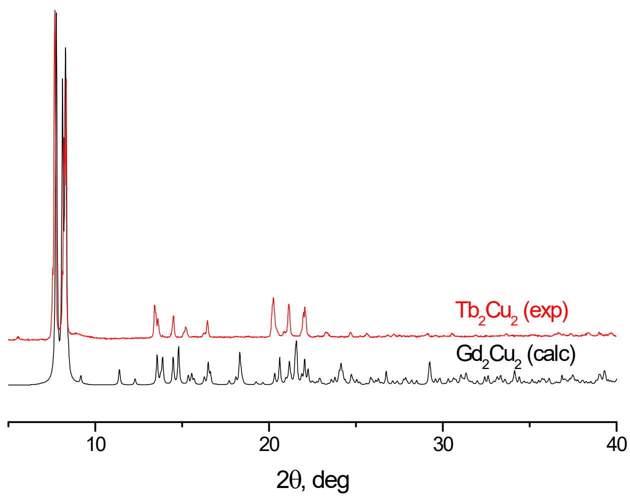
Tb$_2$Cu$_2$ (exp)
Gd$_2$Cu$_2$ (calc)
10
20
30
40
2θ, deg

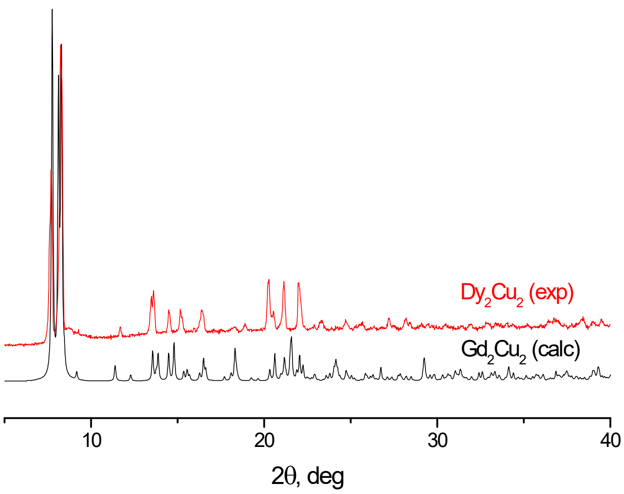
Dy$_2$Cu$_2$ (exp)
Gd$_2$Cu$_2$ (calc)
10
20
30
40
2θ, deg

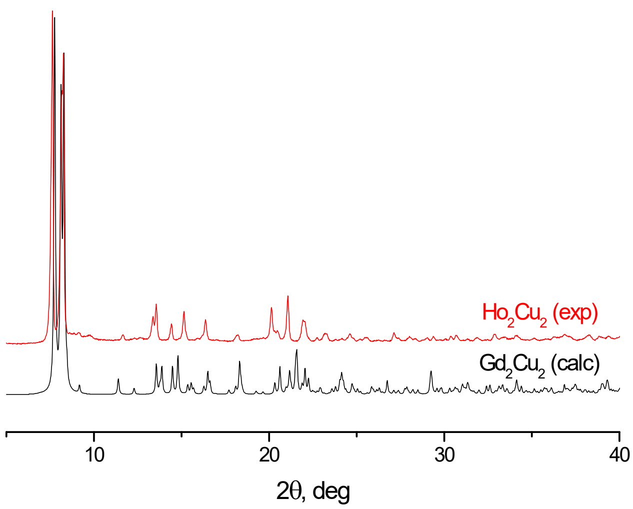
Ho$_2$Cu$_2$ (exp)
Gd$_2$Cu$_2$ (calc)
10
20
30
40
2θ, deg

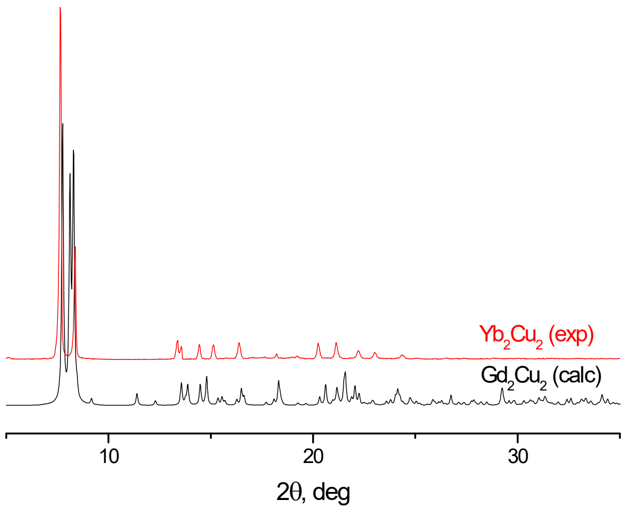

Fig. S1. Experimental PXRD patterns for a series of $\mathbf{1_{Ln}}$ (Ln = Gd, Tb, Dy, Ho, Yb) measured at 273 K and their comparison with calculated data for $\mathbf{1_{Gd}}$.

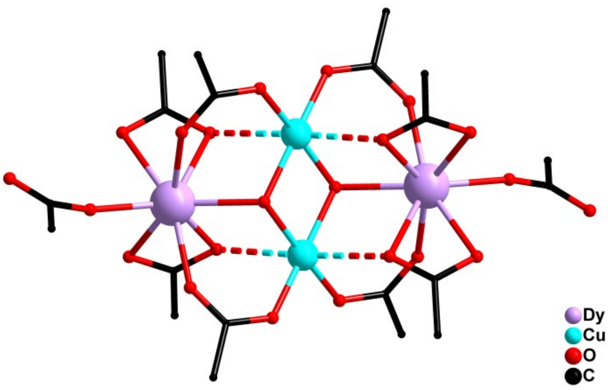

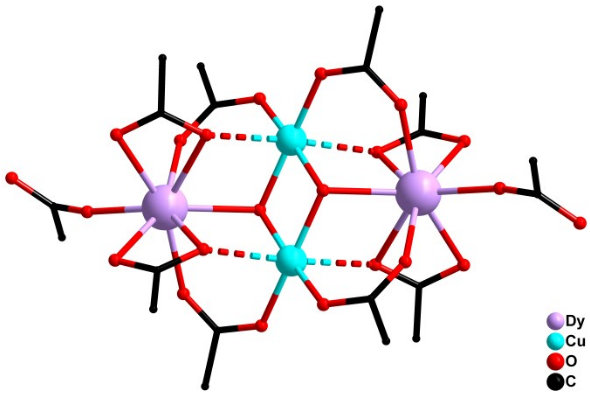

	$\mathbf{2_{Dy}}$	$\mathbf{({}^{i}Pr_2NH_2)_2[Cu_2Dy_2(OH)_2(piv)_{10}]}$
Cu–O(piv), Å	1.942(2), 1.947(2)	1.954
Cu---O(piv), Å	2.568(3), 2.537(3)	2.398, 2.421
Cu–O(μ_3-OH), Å	1.966(2) Å, 1.969(2)	1.978
Dy–O(piv), Å	2.254(2)–2.452(2)	2.244–2.478
Dy–O(μ_3-OH), Å	2.337(2)	2.380
Cu···Cu, Å	3.0371(8)	3.048
Cu···Dy, Å	3.5090(5), 3.5104(6)	3.481, 3.525
Cu–O–Dy,	108.8, 109.0	105.6, 107.6
Cu–O–Cu,	101.0°	100.8°

Fig. S2. Comparison of geometric parameters of the tetranuclear anionic fragments of $\mathbf{2_{Dy}}$ and published complex $({}^{i}Pr_2NH_2)_2[Cu_2Dy_2(OH)_2(piv)_{10}]$.

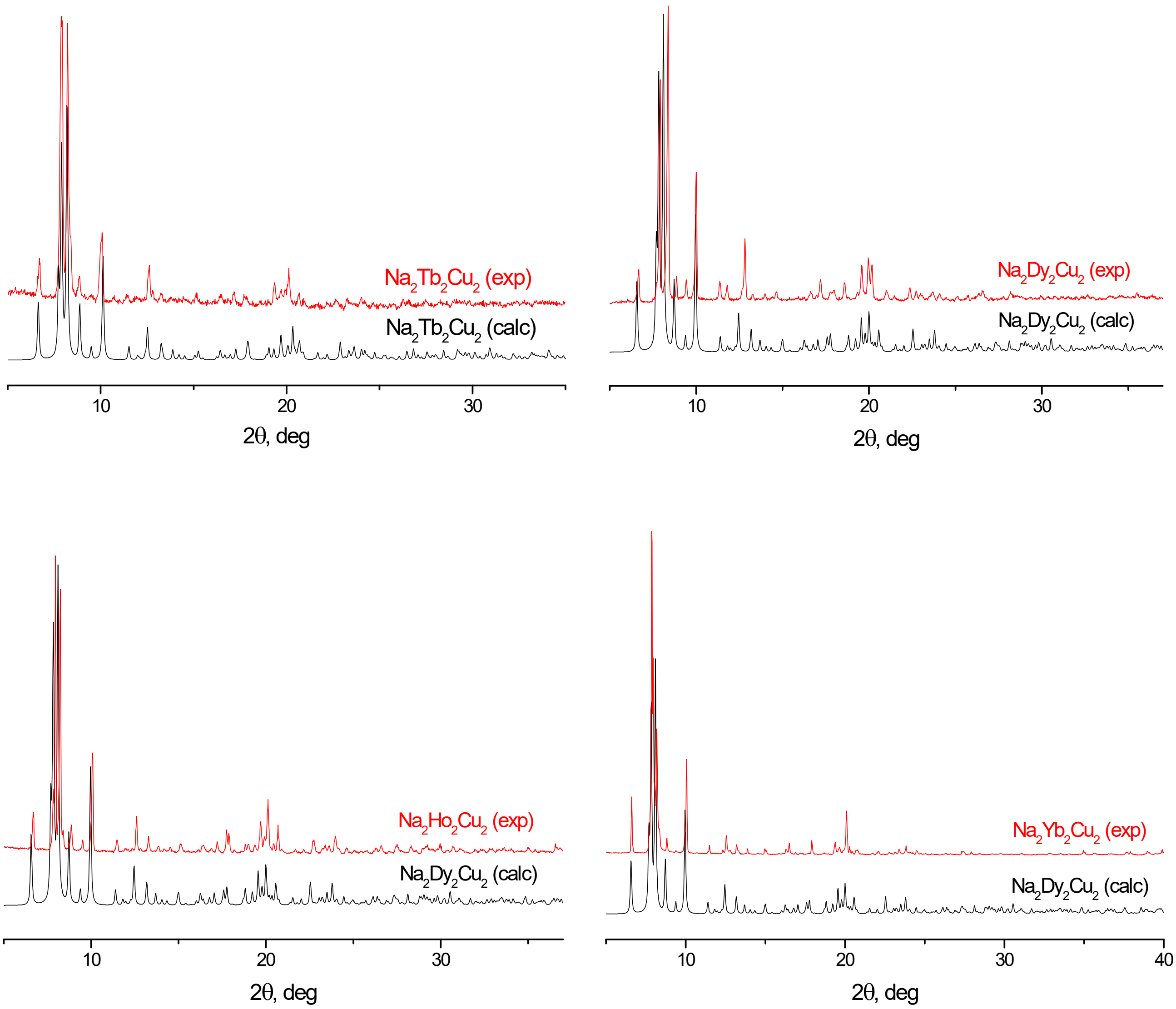

Fig. S3. Experimental PXRD patterns for a series of $\mathbf{2_{Ln}}$ (Ln = Tb, Dy, Ho, Yb) measured at 273 K and their comparison with calculated data for $\mathbf{2_{Tb}}$ (for $\mathbf{2_{Tb}}$) and $\mathbf{2_{Dy}}$ (for $\mathbf{2_{Dy}}$, $\mathbf{2_{Ho}}$, $\mathbf{2_{Yb}}$).

II. Magnetic measurements

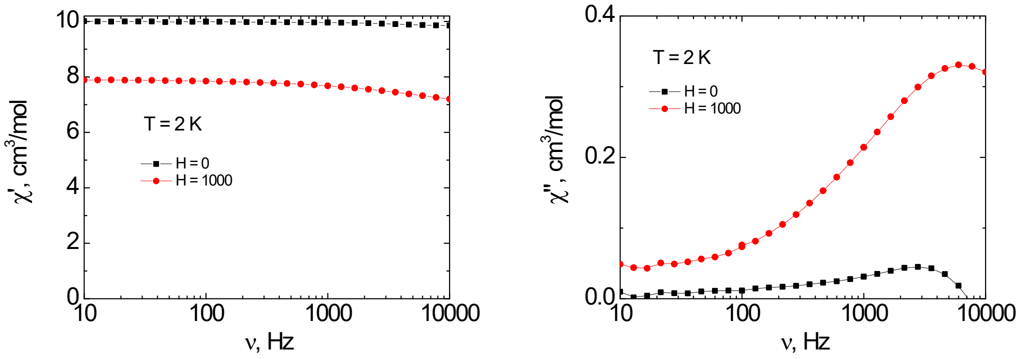

Fig. S4. Frequency dependencies of real, χ' (left) and imaginary, χ'' (right) components of dynamic magnetic susceptibility for complex $\mathbf{1}_{\mathbf{Tb}}$ at $T = 2$ K under various *dc* magnetic fields (Oe). Solid lines are visual guides.

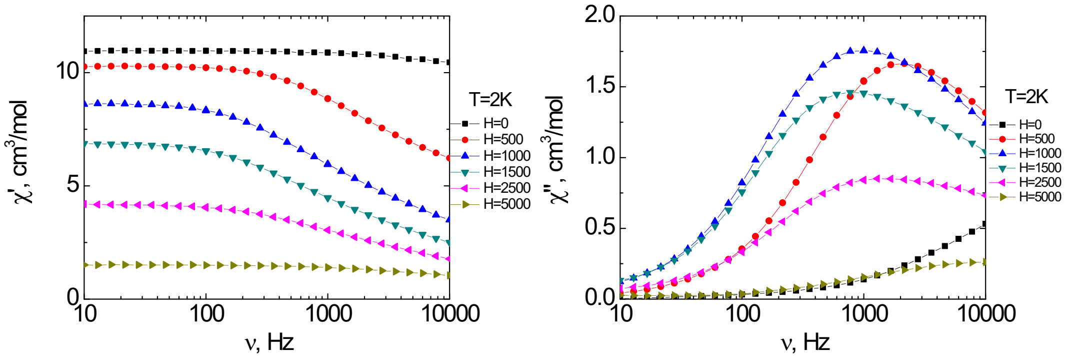

Fig. S5. Frequency dependencies of real, χ' (left) and imaginary, χ'' (right) components of dynamic magnetic susceptibility for complex $\mathbf{1}_{\mathbf{Dy}}$ at $T = 2$ K under various *dc* magnetic fields (Oe). Solid lines are visual guides.

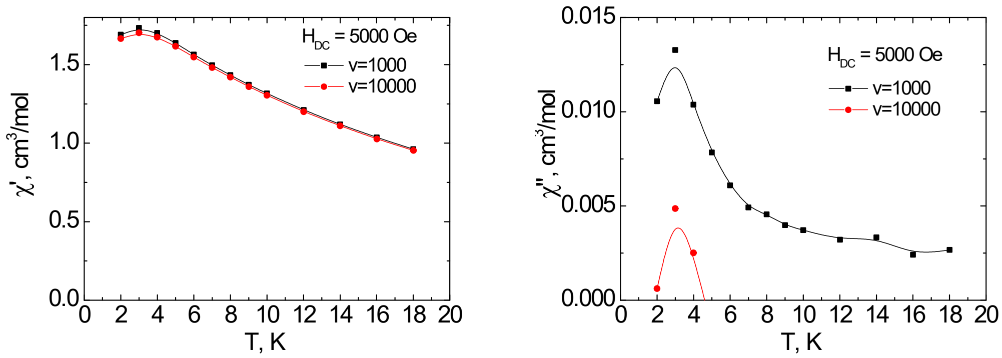

Fig. S6. Frequency dependencies of real, χ' (left) and imaginary, χ'' (right) components of dynamic magnetic susceptibility for complex $\mathbf{1}_{\mathbf{Ho}}$ under $H = 5000$ Oe at temperatures from 18 to 2 K. Solid lines are visual guides.

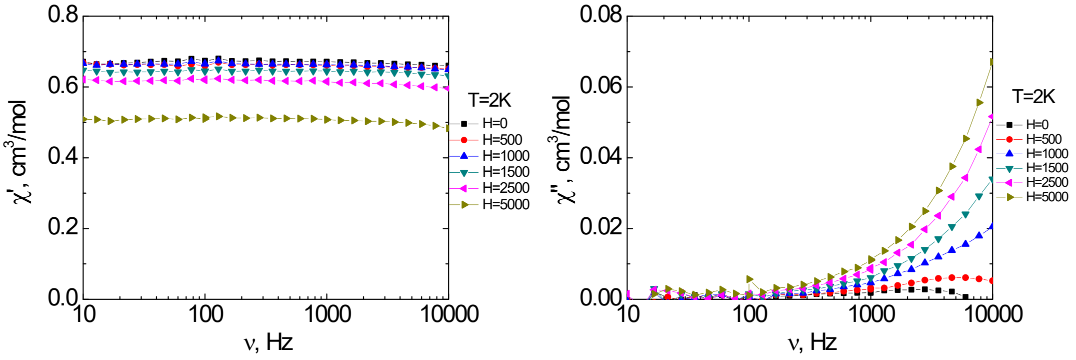

Fig. S7. Frequency dependencies of real, χ' (left) and imaginary, χ'' (right) components of dynamic magnetic susceptibility for complex $\mathbf{1_{Yb}}$ at T = 2 K under various *dc* magnetic fields (Oe). Solid lines are visual guides.

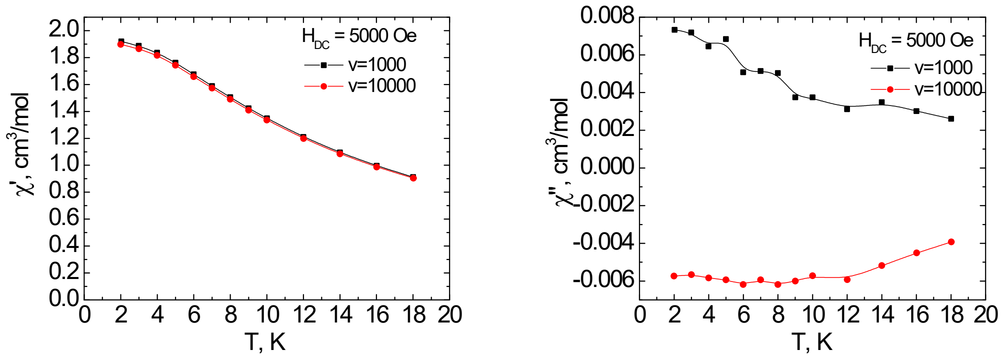

Fig. S8. Frequency dependencies of real, χ' (left) and imaginary, χ'' (right) components of dynamic magnetic susceptibility for complex $\mathbf{2_{Tb}}$ under H = 5000 Oe at temperatures from 18 to 2 K. Solid lines are visual guides.

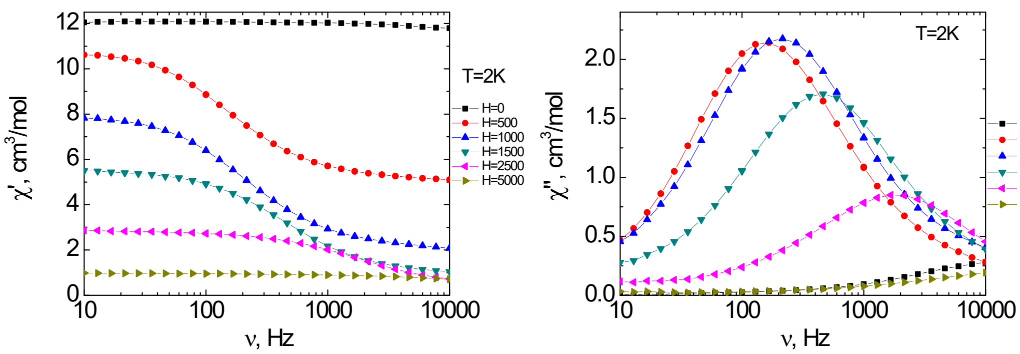

Fig. S9. Frequency dependencies of real, χ' (left) and imaginary, χ'' (right) components of dynamic magnetic susceptibility for complex $\mathbf{2_{Dy}}$ at T = 2 K under various *dc* magnetic fields (Oe). Solid lines are visual guides.

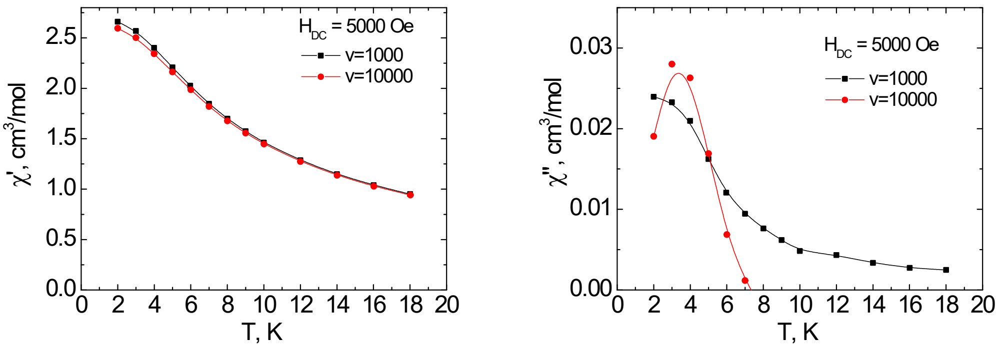

Fig. S10. Frequency dependencies of real, χ' (left) and imaginary, χ'' (right) components of dynamic magnetic susceptibility for complex $\mathbf{2_{Ho}}$ under $H = 5000$ Oe at temperatures from 18 to 2 K. Solid lines are visual guides.

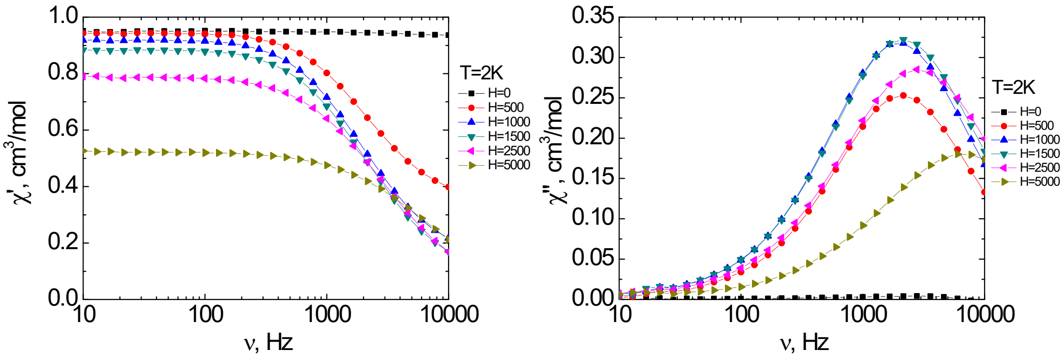

Fig. S11. Frequency dependencies of real, χ' (left) and imaginary, χ'' (right) components of dynamic magnetic susceptibility for complex $\mathbf{2_{Yb}}$ at $T = 2$ K under various *dc* magnetic fields (Oe). Solid lines are visual guides.

Table S9. Fitting of the τ *vs.* T dependences for $\mathbf{1_{Dy}}$.

<table>
<tr><td>Dependence of the relaxation time τ on the reciprocal temperature for $\mathbf{1_{Dy}}$ (H = 1500 Oe, T = 2–4.2 K).</td><td>Fit function, temperature range, and the best-fit parameters with uncertainties.</td></tr>
<tr><td>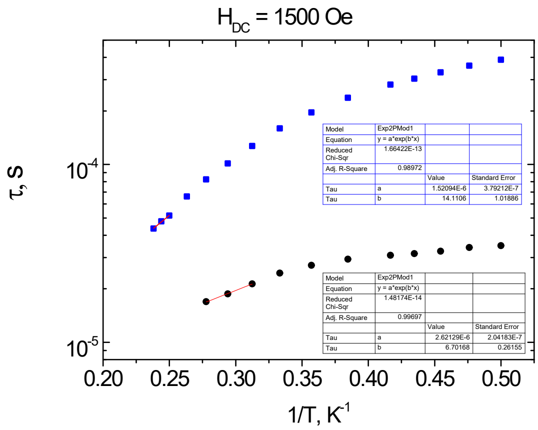
</td><td>Orbach
$\tau = \tau_0 \cdot \exp\{\Delta E/kT\}$

Slow relaxation process (blue dots)

T = 4–4.2 K
$\Delta E/k$ = 14±1 K
$\tau_0 = 1.5 \cdot 10^{-6} \pm 4 \cdot 10^{-7}$ s
R^2 = 0.98972

Fast relaxation process (black dots)

T = 3.2–3.6 K
$\Delta E/k$ = 6.7±0.3 K
$\tau_0 = 2.6 \cdot 10^{-6} \pm 2 \cdot 10^{-7}$ s
R^2 = 0.99697</td></tr>
<tr><td>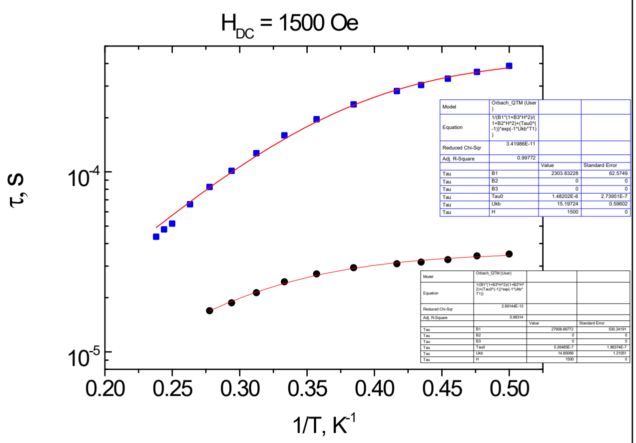
</td><td>Slow relaxation process (blue dots)

Orbach+ QTM
$\tau^{-1} = \tau_0^{-1} \cdot \exp\{-\Delta E/kT\} + B$
T = 2–4.2 K
$\Delta E/k$ = 15.2±0.6 K
$\tau_0 = 1.5 \cdot 10^{-6} \pm 3 \cdot 10^{-7}$ s
B = 2304± 63 s^{-1}
R^2 = 0.99772

Fast relaxation process (black dots)

Orbach+ QTM
$\tau^{-1} = \tau_0^{-1} \cdot \exp\{-\Delta E/kT\} + B$
T = 2–3.6 K
$\Delta E/k$ = 15±1 K
$\tau_0 = 5 \cdot 10^{-7} \pm 2 \cdot 10^{-7}$ s
B = 27959± 530 s^{-1}
R^2 = 0.99314</td></tr>
<tr><td>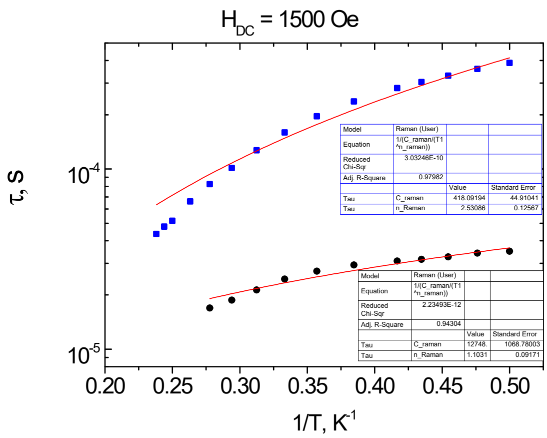
</td><td>Slow relaxation process (blue dots)

Raman
$\tau^{-1} = C_{Raman} T^{n\_Raman}$
T = 2–4.2 K
C_{Raman}= 418±45 $s^{-1}K^{-n\_Raman}$
n_Raman= 2.5±0.1
R^2 = 0.97982</td></tr>
</table>

Fast relaxation process (black dots)

Raman

$\tau^{-1} = C_{Raman}T^{n\_Raman}$

T = 2–3.6 K

C_{Raman}= 12748±1069 $s^{-1}K^{-n\_Raman}$

n_Raman= 1.10±0.09

R^2 = 0.94304

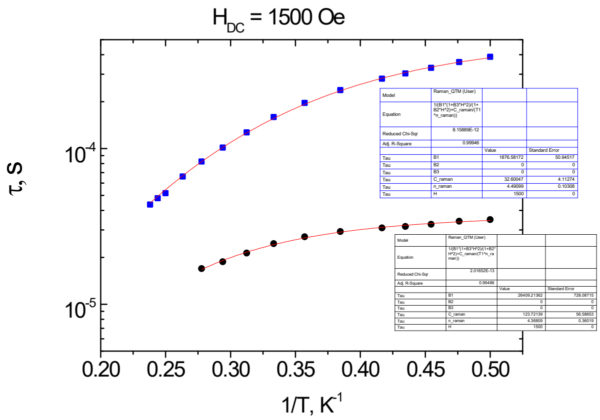

Slow relaxation process (blue dots)

Raman+ QTM

$\tau^{-1} = C_{Raman}T^{n\_Raman} + B$

T = 2–4.2 K

C_{Raman}= 33±4 $s^{-1}K^{-n\_Raman}$

n_Raman= 4.5±0.1

B = 1877±51 s^{-1}

R^2 = 0.99946

Fast relaxation process (black dots)

Raman+ QTM

$\tau^{-1} = C_{Raman}T^{n\_Raman} + B$

T = 2–3.6 K

C_{Raman}= 124±56 $s^{-1}K^{-n\_Raman}$

n_Raman= 4.4±0.4

B = 26409±728 s^{-1}

R^2 = 0.99486

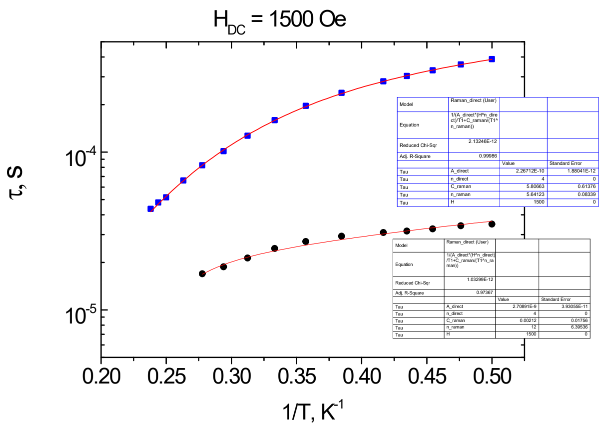

Slow relaxation process (blue dots)

Raman+Direct

$\tau^{-1} = C_{Raman}T^{n\_Raman} + A_{direct}TH^4$

T = 2–4.2 K

C_{Raman}= 5.8±0.6 $s^{-1}K^{-n\_Raman}$

n_Raman= 5.64±0.08

A_{direct} = 2.27·10^{-10}±2·10^{-12} $K^{-1}Oe^{-4}s^{-1}$

R^2 = 0.99986

Fast relaxation process (black dots)

Raman+Direct

$\tau^{-1} = C_{Raman}T^{n\_Raman} + A_{direct}TH^4$

T = 2–3.6 K

C_{Raman}= 0.002±0.018 $s^{-1}K^{-n\_Raman}$

n_Raman= 12±6

A_{direct} = 2.71·10^{-9}±4·10^{-11} $K^{-1}Oe^{-4}s^{-1}$

R^2 = 0.97367

Over-parametrization

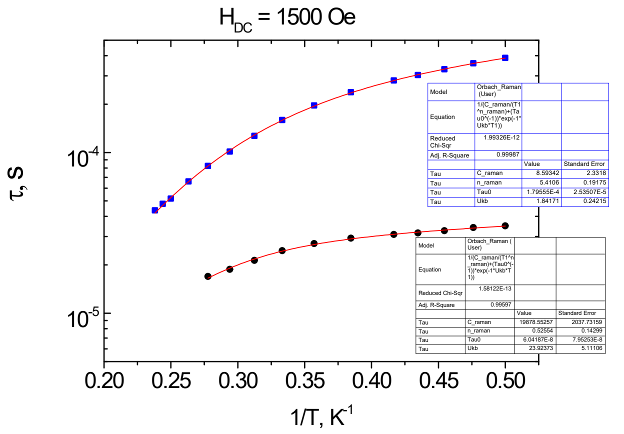

Slow relaxation process (blue dots)

Orbach+Raman

$\tau^{-1} = \tau_0^{-1} \cdot \exp\{-\Delta E/kT\} + C_{Raman} T^{n\_Raman}$

T = 2–4.2 K

$\Delta E/k$ = 1.8±0.2 K

$\tau_0 = 1.8 \cdot 10^{-4} \pm 3 \cdot 10^{-5}$ s

C_{Raman}= 9±2 $s^{-1}K^{-n\_Raman}$

n_Raman= 5.4±0.2

R^2 = 0.99987

Fast relaxation process (black dots)

Orbach+Raman

$\tau^{-1} = \tau_0^{-1} \cdot \exp\{-\Delta E/kT\} + C_{Raman} T^{n\_Raman}$

T = 2–3.6 K

$\Delta E/k$ = 24±5 K

$\tau_0 = 6 \cdot 10^{-8} \pm 8 \cdot 10^{-8}$ s

C_{Raman}= 19879±2038 $s^{-1}K^{-n\_Raman}$

n_Raman= 0.5±0.1

R^2 = 0.99597

Over-parametrization

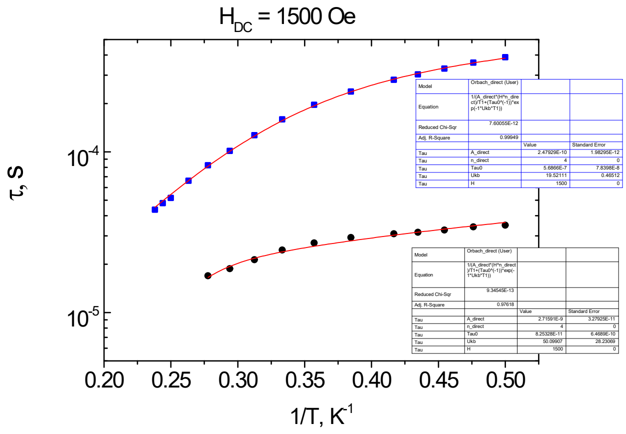

Slow relaxation process (blue dots)

Orbach+Direct

$\tau^{-1} = \tau_0^{-1} \cdot \exp\{-\Delta E/kT\} + A_{direct} T H^4$

T = 2–4.2 K

$\Delta E/k$ = 19.5±0.5 K

$\tau_0 = 5.7 \cdot 10^{-7} \pm 8 \cdot 10^{-8}$ s

$A_{direct} = 2.48 \cdot 10^{-10} \pm 2 \cdot 10^{-12}$ $K^{-1}Oe^{-4}s^{-1}$

R^2 = 0.99949

Fast relaxation process (black dots)

Orbach+Direct

$\tau^{-1} = \tau_0^{-1} \cdot \exp\{-\Delta E/kT\} + A_{direct} T H^4$

T = 2–3.6 K

$\Delta E/k$ = 50±28 K

$\tau_0 = 8 \cdot 10^{-11} \pm 6 \cdot 10^{-10}$ s

$A_{direct} = 2.72 \cdot 10^{-9} \pm 3 \cdot 10^{-11}$ $K^{-1}Oe^{-4}s^{-1}$

R^2 = 0.97618

Over-parametrization

Table S10. Fitting of the τ *vs.* *T* dependences for $\mathbf{2_{Dy}}$.

Dependence of the relaxation time τ on the reciprocal temperature for $\mathbf{2_{Dy}}$ (H = 500 Oe, T = 2–3.5 K).	Fit function, temperature range, and the best-fit parameters with uncertainties.
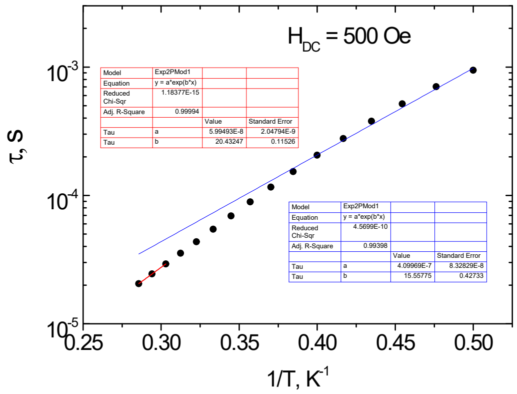	**Orbach** $\tau = \tau_0 \cdot \exp\{\Delta E/kT\}$ T = 3.3–3.5 K $\Delta E/k$ = 20.4±0.1 K $\tau_0 = 6.0 \cdot 10^{-8} \pm 2 \cdot 10^{-9}$ s R^2 = 0.99994 (red line) T = 2–3.5 K $\Delta E/k$ = 15.6±0.4 K $\tau_0 = 4.1 \cdot 10^{-7} \pm 8 \cdot 10^{-8}$ s R^2 = 0.99398 (blue line)
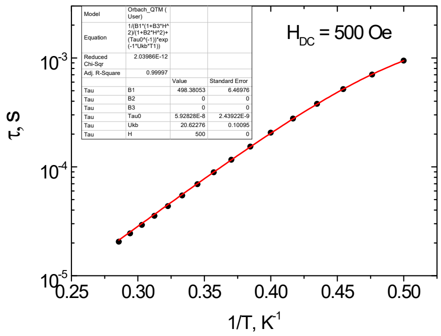	**Orbach+ QTM** $\tau^{-1} = \tau_0^{-1} \cdot \exp\{-\Delta E/kT\} + \mathrm{B}$ T = 2–3.5 K $\Delta E/k$ = 20.6±0.1 K $\tau_0 = 5.9 \cdot 10^{-8} \pm 2 \cdot 10^{-9}$ s B = 498± 6 s^{-1} R^2 = 0.99997
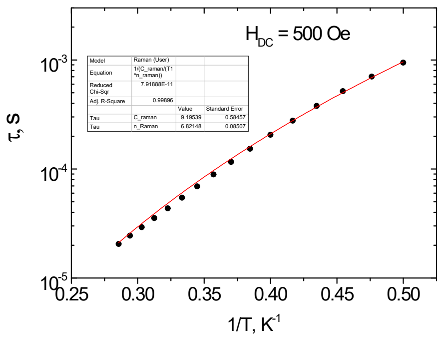	**Raman** $\tau^{-1} = C_{Raman} T^{n\_Raman}$ T = 2–3.5 K C_{Raman}= 9.2±0.6 $s^{-1}K^{-n\_Raman}$ n_Raman= 6.82±0.09 R^2 = 0.99896
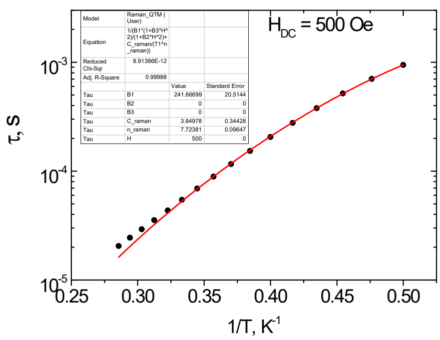	**Raman+ QTM** $\tau^{-1} = C_{Raman} T^{n\_Raman} + \mathrm{B}$ T = 2–3.5 K C_{Raman}= 3.8±0.3 $s^{-1}K^{-n\_Raman}$ n_Raman= 7.7±0.1 B = 242±21 s^{-1} R^2 = 0.99988

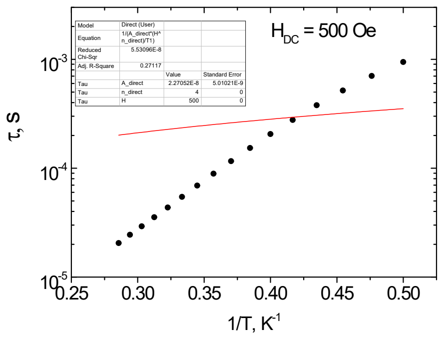

Direct

$\tau^{-1} = A_{direct}TH^4$

$T = 2–3.5$ K

$A_{direct} = 2.3\cdot10^{-8}\pm5\cdot10^{-9}$ K^{-1}Oe^{-4}s^{-1}

$R^2 = 0.27117$

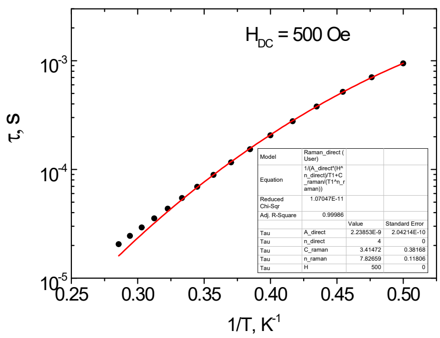

Raman+Direct

$\tau^{-1} = C_{Raman}T^{n\_Raman} + A_{direct}TH^4$

$T = 2–3.5$ K

$C_{Raman} = 3.4\pm0.4$ s^{-1}K$^{-n_Raman}$

n_Raman= 7.8±0.1

$A_{direct} = 2.2\cdot10^{-9}\pm2\cdot10^{-10}$ K^{-1}Oe^{-4}s^{-1}

$R^2 = 0.99986$

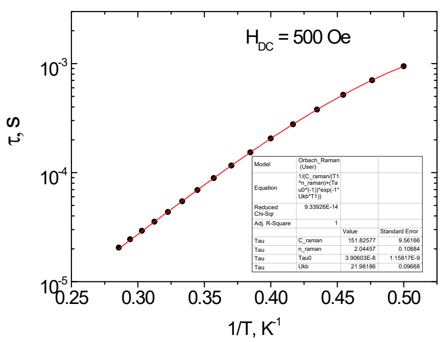

Orbach+Raman

$\tau^{-1} = \tau_0^{-1}\cdot\exp\{-\Delta E/kT\} + C_{Raman}T^{n\_Raman}$

$T = 2–3.5$ K

$\Delta E/k = 22.0\pm0.1$ K

$\tau_0 = 3.9\cdot10^{-8}\pm1\cdot10^{-9}$ s

$C_{Raman} = 152\pm10$ s^{-1}K$^{-n_Raman}$

n_Raman= 2.0±0.1

$R^2 = 1$

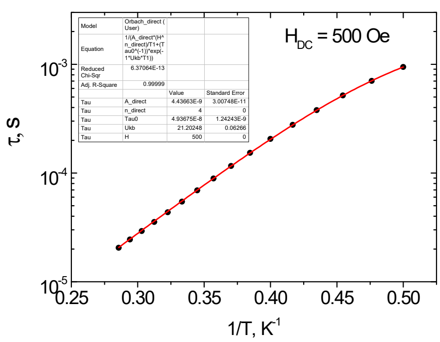

Orbach+Direct

$\tau^{-1} = \tau_0^{-1}\cdot\exp\{-\Delta E/kT\} + A_{direct}TH^4$

$T = 2–3.5$ K

$\Delta E/k = 21.20\pm0.06$ K

$\tau_0 = 4.9\cdot10^{-8}\pm1\cdot10^{-9}$ s

$A_{direct} = 4.44\cdot10^{-9}\pm3\cdot10^{-11}$ K^{-1}Oe^{-4}s^{-1}

$R^2 = 0.99999$

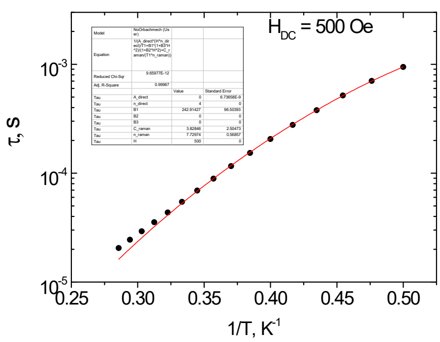

Raman+Direct+QTM

$\tau^{-1} = C_{Raman}T^{n\_Raman} + B + A_{direct}TH^4$

$T = 2–3.5$ K

$A_{direct} = 0\pm7\cdot10^{-9}$ K^{-1}Oe^{-4}s^{-1}

$C_{Raman} = 4\pm3$ s^{-1}K$^{-n_Raman}$

n_Raman= 7.7±0.6

B = 243±97 s^{-1}

$R^2 = 0.99987$

Over-parametrization

Table S11. Fitting of the τ *vs.* T and τ *vs.* H dependences for $\mathbf{2_{Dy}}$.

Dependences of the relaxation time τ on the reciprocal temperature and field for $\mathbf{2_{Dy}}$ (H = 500 Oe, T = 2–3.5 K).	Fit function, temperature range, and the best-fit parameters with uncertainties.
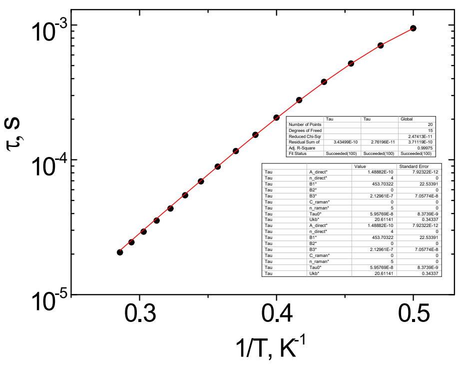 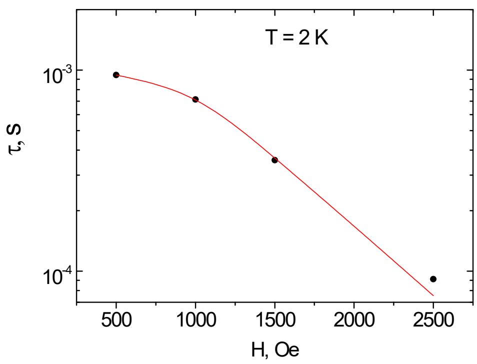	**Orbach+Direct+QTM** *Simultaneous fit* $\tau^{-1} = \tau_0^{-1} \cdot \exp\{-\Delta E/kT\} + B_1 \cdot (1+B_3 \cdot H^2) + A_{direct} T H^4$ T = 2-3.5 K; H = 500-2500 Oe $A_{direct} = 1.49 \cdot 10^{-10} \pm 8 \cdot 10^{-12}$ K^{-1}Oe^{-4}s^{-1} $B_1 = 454 \pm 23$ s^{-1} $B_3 = 2.1 \cdot 10^{-7} \pm 7 \cdot 10^{-8}$ Oe^{-2} $\Delta E/k = 20.6 \pm 0.3$ K $\tau_0 = 6.0 \cdot 10^{-8} \pm 8 \cdot 10^{-9}$ s $R^2 = 0.99975$

Table S12. Fitting of the τ *vs.* *T* dependences for $\mathbf{2_{Yb}}$

<table>
<tr>
<td>Dependence of the relaxation time τ on the reciprocal temperature for $\mathbf{2_{Yb}}$ (H = 1000 Oe, T = 2–4 K).</td>
<td>Fit function, temperature range, and the best-fit parameters with uncertainties.</td>
</tr>
<tr>
<td>
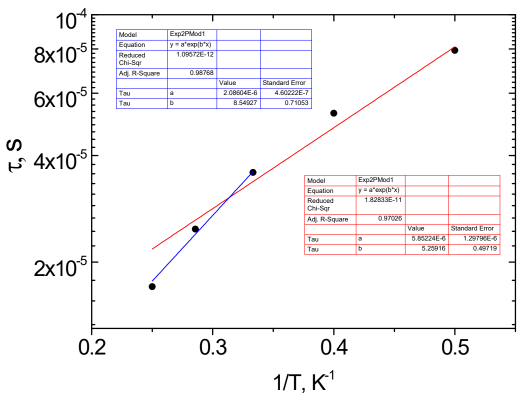

</td>
<td>
Orbach
$\tau = \tau_0 \cdot \exp\{\Delta E/kT\}$
T = 3–4 K
$\Delta E/k$ = 8.5±0.7 K
$\tau_0 = 2.1 \cdot 10^{-6} \pm 5 \cdot 10^{-7}$ s
R^2 = 0.98768 (blue line)

T = 2-4 K
$\Delta E/k$ = 5.3±0.5 K
$\tau_0 = 6 \cdot 10^{-6} \pm 1 \cdot 10^{-6}$ s
R^2 = 0.97026 (red line)
</td>
</tr>
<tr>
<td>
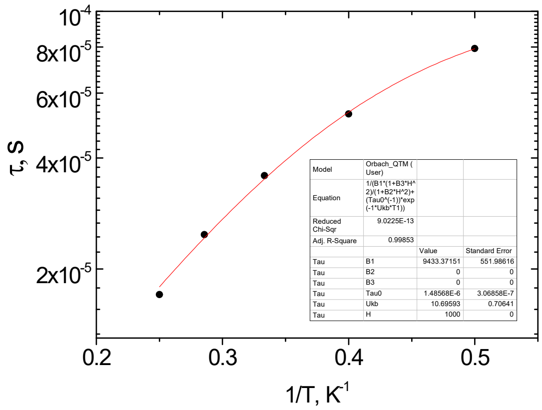

</td>
<td>
Orbach+ QTM
$\tau^{-1} = \tau_0^{-1} \cdot \exp\{-\Delta E/kT\} + \mathrm{B}$
T = 2-4 K
$\Delta E/k$ = 10.7±0.7 K
$\tau_0 = 1.5 \cdot 10^{-6} \pm 3 \cdot 10^{-7}$ s
B = 9433± 552 s^{-1}
R^2 = 0.99853
</td>
</tr>
<tr>
<td>
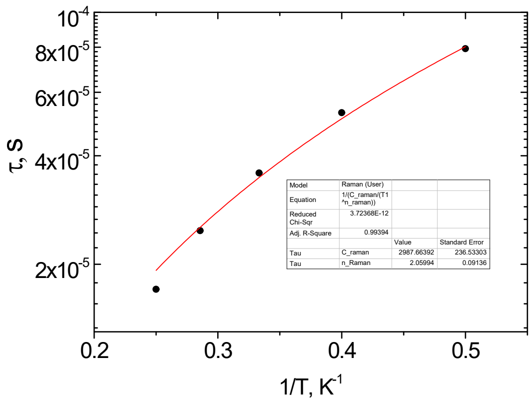

</td>
<td>
Raman
$\tau^{-1} = C_{Raman} T^{n\_Raman}$
T = 2-4 K
C_{Raman}= 2988±237 $s^{-1}K^{-n\_Raman}$
n_Raman= 2.06±0.09
R^2 = 0.99394
</td>
</tr>
</table>

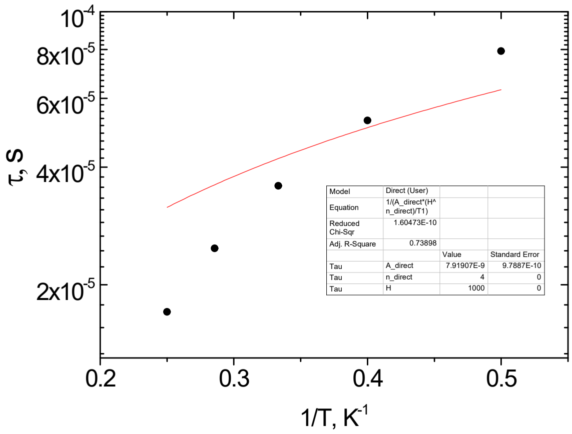

Direct

$\tau^{-1} = A_{direct}TH^4$

T = 2-4 K

$A_{direct} = 8\cdot10^{-9}\pm1\cdot10^{-9}$ K^{-1}Oe^{-4}s^{-1}

$R^2 = 0.73898$

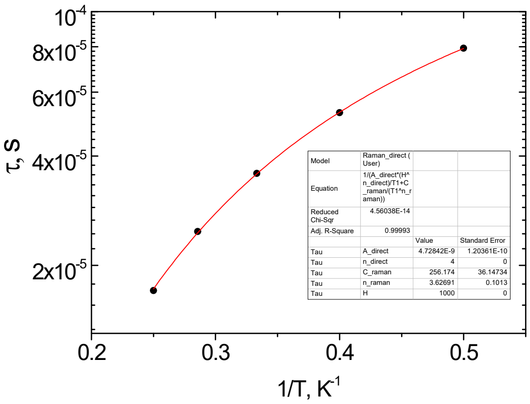

Raman+Direct

$\tau^{-1} = C_{\mathrm{Raman}}T^{\mathrm{n\_Raman}} + A_{direct}TH^4$

T = 2-4 K

C_{Raman} = 256±36 s^{-1}K$^{-\mathrm{n_Raman}}$

n_Raman = 3.6±0.1

$A_{direct} = 4.7\cdot10^{-9}\pm1\cdot10^{-10}$ K^{-1}Oe^{-4}s^{-1}

$R^2 = 0.99993$

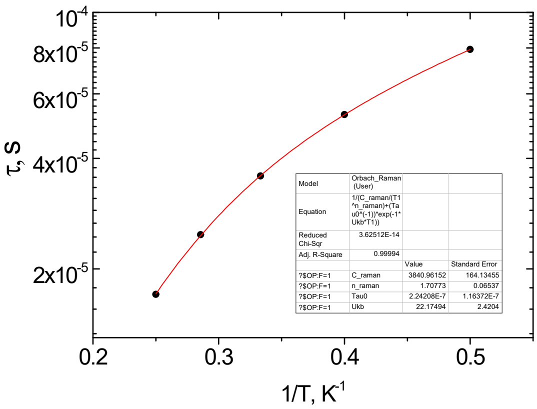

Orbach+Raman

$\tau^{-1} = \tau_0^{-1}\cdot\exp\{-\Delta E/kT\} + C_{\mathrm{Raman}}T^{\mathrm{n\_Raman}}$

T = 2-4 K

$\Delta E/k$ = 22±2 K

$\tau_0 = 2\cdot10^{-7}\pm1\cdot10^{-7}$ s

C_{Raman} = 3841±164 s^{-1}K$^{-\mathrm{n_Raman}}$

n_Raman = 1.71±0.07

$R^2 = 0.99994$

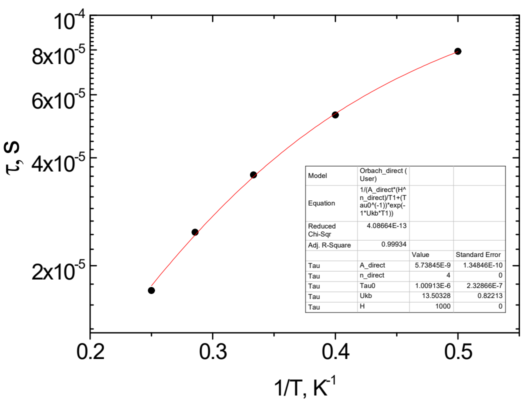

Orbach+Direct

$\tau^{-1} = \tau_0^{-1}\cdot\exp\{-\Delta E/kT\} + A_{direct}TH^4$

T = 2-4 K

$\Delta E/k$ = 13.5±0.8 K

$\tau_0 = 1.0\cdot10^{-6}\pm2\cdot10^{-7}$ s

$A_{direct} = 5.7\cdot10^{-9}\pm1\cdot10^{-10}$ K^{-1}Oe^{-4}s^{-1}

$R^2 = 0.99934$

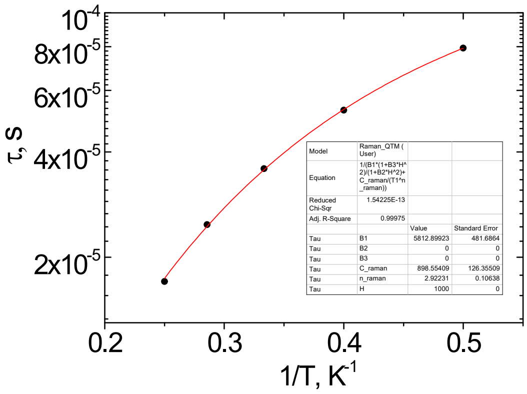

Raman+QTM

$\tau^{-1} = C_{\mathrm{Raman}} T^{\mathrm{n\_Raman}} + \mathrm{B}$

T = 2-4 K

C_{Raman}= 899±126 $\mathrm{s}^{-1}\mathrm{K}^{-\mathrm{n\_Raman}}$

n_Raman= 2.9±0.1

B = 5813± 482 s^{-1}

R^2 = 0.99975

Table S13. Fitting of the τ *vs.* T and τ *vs.* H dependences for $\mathbf{2_{Yb}}$.

<table>
<tr>
<td>Dependences of the relaxation time τ on the reciprocal temperature and field for $\mathbf{2_{Yb}}$ (H = 1000 Oe, T = 2–4 K).</td>
<td>Fit function, temperature range, and the best-fit parameters with uncertainties.</td>
</tr>
<tr>
<td>
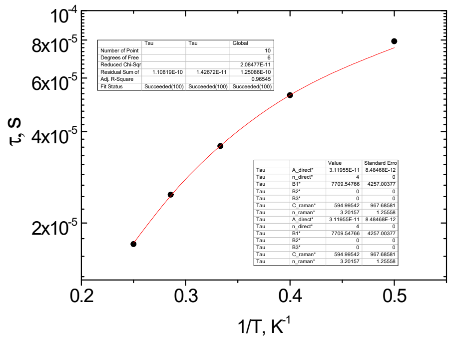

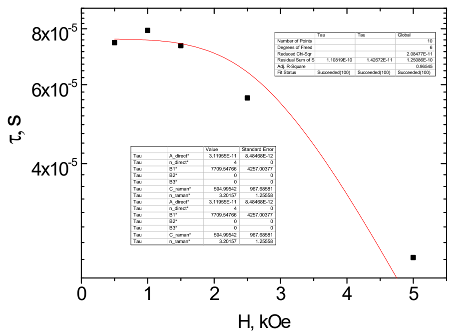

</td>
<td>
Raman+Direct+QTM

Simultaneous fit

$\tau^{-1} = \tau_0^{-1}\cdot\exp\{-\Delta E/kT\} + B + A_{direct}TH^4$

Formulas with a greater number of parameters of QTM do not lead to better approximation.

T = 2-4 K; H = 500-5000 Oe

C_{Raman}= 595±968 $s^{-1}K^{-n\_Raman}$
n_Raman= 3±1

$A_{direct} = 3.1\cdot10^{-11}\pm8\cdot10^{-12}$ $K^{-1}Oe^{-4}s^{-1}$

B = 7710±4257 s^{-1}

R^2 = 0.96545
</td>
</tr>
</table>